ANISOTROPIC BEHAVIOR OF TAGE TUFF IN CHANGING SATURATION

A.M.N. Madurya ADIKARAM[1)], Masahiko OSADA[1)] and Tadashi YAMABE[1)]
[1)] Rock Mechanics Lab., Department of Civil and Environmental Engineering, Saitama University

ABSTRACT

The study was conducted to identify the anisotropic behavior of Tage tuff with heat and in changing saturations. Ultrasonic wave based technique was used to identify the anisotropic dynamic mechanical properties of Tage tuff in heated and unheated conditions with saturation. The heated dry samples show high dynamic elastic properties and heated saturated samples show comparatively low elastic properties. Vacuum saturated tuff in unheated condition shows highest dynamic elastic properties due to patchy saturation. MIP test was done for the above sample conditions and identified the porosity is not changing with heating, but the pore size distribution is changed with heating. Strain and ultrasonic wave velocity were measured concurrently to obtain the deformation in changing saturations. The P wave velocity is decreasing and S wave velocity is constant with constant strains when the samples dry from fully saturation. In below saturations of around 30%, both velocities increased with decrease in strains. This effect was modified using theories of poroelasticity. Therefore, it can be concluded the Tage tuff has desiccation driven hardening characteristic which depends on the bedding plane.

KEYWORDS: Tage tuff, transversely isotropic, saturation, dynamic mechanical properties, strain

1. INTRODUCTION

A major challenge of rock mechanics is to identify the mechanisms and deformations of sedimentary rocks which can be applied to the scientific inventions and the development of the world. Sedimentary rocks cover about 66% of the earth's continental surface (Blatt et al., 2006). Sedimentary rocks are formed due to the sedimentation, compaction and cementation of minerals or organic material on the earth surface or under water bodies. The rock formation conditions (especially temperature and pressure) are low with compare to the other two major rock types (igneous and metamorphic) and therefore sedimentary rocks are comparatively less in strength. As a result, manmade surface structures on sedimentary rocks are readily affected with the changing atmospheric environment and, many mechanisms such as weathering and deformations are happening on them within a short period of the time.

A special concern should be given to underground excavations and deformations of the rocks as they are exposing to a totally different environment with a short time period. The newly exposed surface of an underground excavation is named as Excavation Damaged Zone (EDZ) which acts as the interpreter of the exposed environment and the fresh rock. The rock type, excavation method, dimensions of the excavation, purpose of the excavation, depth to the surface, exposed environmental conditions (pressure, temperature, humidity, etc.) are the factors for the changes of the EDZ. Those changes of the EDZ can make deformations such as new cracks due to pressure releasing, drying effects due to humidity changes and further modification of EDZ due to weakening of the rock.

Considering above matters on sedimentary rocks present study mainly considered about the degree of saturation and effect of heat of a rock as they affect the mechanical properties. The selected rock type is Tage tuff which was obtained from the Tochigi prefecture of Japan. Tuff rock is a kind of sedimentary rock which consists of compacted and welded volcanic ash and dust. Due to origin of the material it is considered as a volcanic rock. However, texturally it belongs to sedimentary class. Tuff rocks contain up to about 50% of the sedimentary material (Blatt et al., 2006). It is a well porous light weight rock. The mineralogy of Tage tuff has being examined by Funatsu et al. in 2004 using XRD method and indicated that it contains clinoptilolite (49.2%), quartz (27.4%), anorthite (8.2%), cristoblite (6.3%) and smectite (3.6%). Several studies have being recorded in the literature considering the stress induced mechanical properties of Tage Tuff (Okubo and Fukui, 1996, Funatsu et al., 2004, Okubo et al., 2008). However, there are lacks of studies considering the drying induced deformations of tuff rocks under no stress conditions (Aung et al., 2008) and present study extended this to Tage tuff considering the

anisotropy also.

In order to consider rock conditions as simple, rocks are considered as elastic and isotropic materials. However, real properties of rocks are differing from the above conditions. Several experiments have being done under applied confining pressure to obtain the mechanical properties of anisotropic rocks (King, 1969, King, 2000, Lo et al., 1986). It was identified Tage tuff has transversely isotropic properties with the consideration of the drying and strain measurement done on parallel and perpendicular directions to the bedding plane (Adikaram et al., 2010). Therefore, first part of the study concerns investigation of dynamic mechanical properties of transversely isotropic Tage tuff in no confining pressures.

The second part of the study is to identify the relationship of ultrasonic wave velocities and saturation. Previous studies identified some of the changes of wave velocities with saturation based on ultrasonic measuring techniques for different rock types (Wyllie et al., 1956, Konstantinova et al., 1980, King et al., 2000, Wang et al., 2005, Kahraman, 2007, King, 2009, Ghorbani et al. 2009). Present study extended it to transversely isotropic sedimentary rock, Tage tuff.

2. METHODS

A large block of Tage tuff was used and cut the cylindrical samples with the axis of the sample is parallel, perpendicular and 45 degrees inclined to the bedding plane. Eight samples were cut for each bedding alignment and the selected sample height and diameter was 3cm and 5cm respectively.

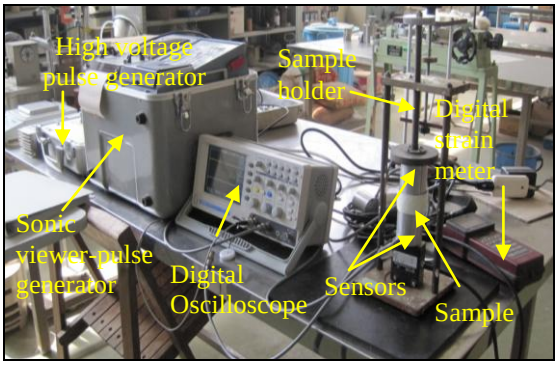

Figure 1 Instrument setup for velocity measurement

First part of the experiment was to identify the dynamic mechanical properties for two different conditions as heated in to 105°C for 48 hours in the electric oven and non heated samples in the laboratory environmental condition. Mechanical properties were checked on dry and vacuum saturated samples in room temperature. The ultrasonic transmission method was used to measure the wave velocities of each rock sample. Compressional and shear wave travel times were measured along the long axis of the cylindrical samples. Vernier calliper was used to measure the sample height along the cylindrical axis. Procedure of the experiment was started with the pulse generator (Sonic Viewer 170 Model 5228) and amplified pulse (High Voltage Pulse Generator Model 5234) was used to generate waves in the transducers (Figure 1). The voltage of the amplifier is 800V and therefore high voltage pulse was used for the measurements. The transducers are with 30 kHz frequency and the working surface of the transducer is 4.5 cm in diameter. Digital oscilloscope was used to obtain the wave forms and manually recorded the data. While measuring the travel time, sample was kept in a sample holder so that a constant force (10kgf) applied to the sample by using a digital strain meter. The velocity (v) is determined as $v=l/t$, where l is the length of the sample and t is the travel time.

Two types of piezoelectric sensors (USD 30 and UPD 30, and S33K and P63K) were used for the clarification of the wave arrival times for P and S waves of the urethane (Ethyl carbamate) test piece and decided the exact arrival time for the samples.

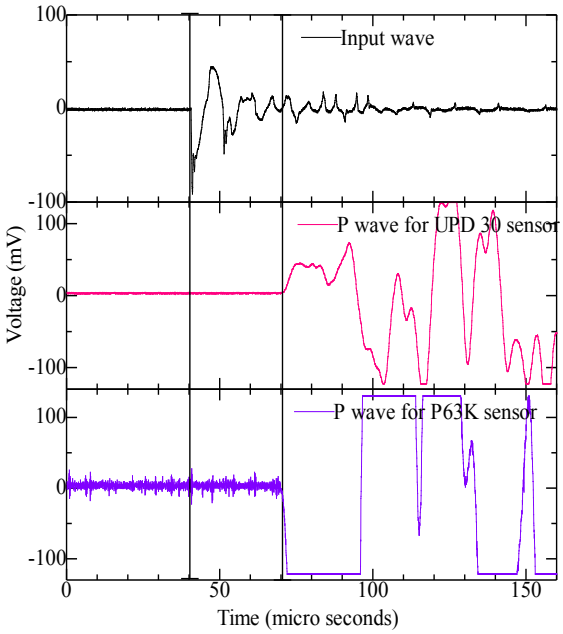

Figure 2 P wave arrival time

Generally, P wave is the fastest arrival wave which was propagated through the earth materials. In P wave, output for the P63K sensor and UPD 30 sensor clearly shows the same point as the breaking point of the wave (Figure 2). Therefore, for P wave arrival time measurements of samples were taken as the first starting point or the first breaking point of the output signal. In literature also several researches have being used the first breaking point as the P wave arrival point (Sawangsuriya et al. 2008, King, 1969, Murillo et al., 2009).

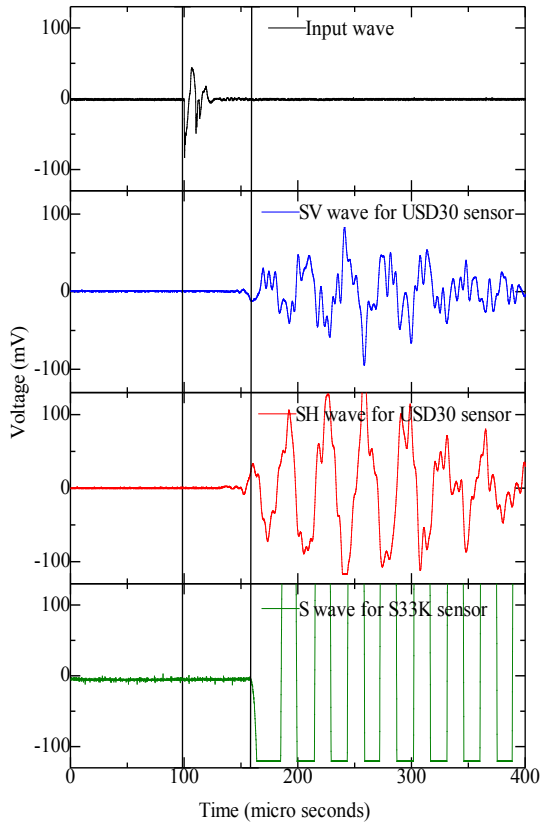

Figure 3 S wave arrival time

The S wave arrival position was selected considering the wave arrival point of urethane which was considered as a homogeneous material and therefore no change in SH and SV wave arrival points despite of polarization. In the literature, several researches have being used several positions as the S wave arrival point (Murillo et al., 2009). It has being done considering the time domain or frequency domain. For example in time domain, as the first inversion of the output signal (Murillo et al., 2009), as the point zero after first inflection of the received signal or the transient point of the polarity (Sawangsuriya et al. 2008) and as the first breaking point of the output signal (King, 1969). In our experiment, the wave breaking point of the S33K sensor is coincided with the first peak point of the wave of USD30 sensor which has significant amplitude with compare to the small wave breaks in the front (Figure 3). Generally, the first small peak is considered as near field effect or the noise and in most cases it is neglecting. In the literature also similar position of the S wave output was taken as the first S wave arrival point (Duttine et al., 2007).

Considering the relevant equations on transversely isotropic rock (King, 1969, Lo et al., 1986, Song et al., 2004, Mavko et al., 2009), Young' moduli, Poisson's ratio and shear moduli were calculated for Tage tuff in dry and saturated condition for heated (105°C) and non heated samples.

In order to examine the porosity and pore size distribution effect on the above experiment Mercury Intrusion Porosimetry (MIP) test was done for different heating temperatures.

Second part of the experiment is to measure the ultrasonic wave velocities and strain with changing saturations. Initially oven dried samples in to 105°C were vacuum saturated to obtain fully saturated condition. Two sets of samples were used for one experiment with same bedding alignment.

Four strain gauges were pasted on one sample as same as Aung et al., 2009, 2010, which can measure strain in perpendicular to the bedding and in two perpendicular directions along the bedding (Figure 4). The other sample was used for the ultrasonic velocity measurements on P and S waves. Both samples were covered using silicon rubber sealant and thin plastic films allowing one dimensional drying in the flat surface as the evaporating surface is parallel to the bedding and perpendicular to the bedding. Samples were kept inside an incubator with 50°C and 50% humidity. Strains and sample weight of the strain measuring sample were recorded in a data logger with 1 minute intervals and velocities and weight of the other sample were recorded manually by taking out the sample in decided time intervals.

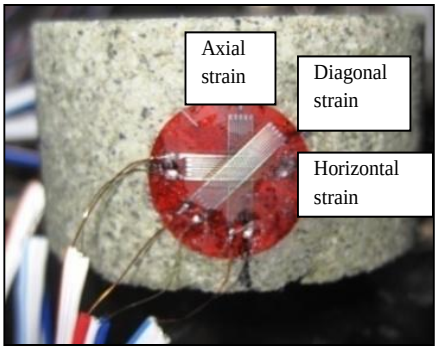

Figure 4 Strain gauge pasted on the sample

3. ESTIMATION OF ANISOTROPIC CONSTANTS

Figure 5 explains a plot of P wave velocity and S wave velocity with density. It can be observed the P wave velocity for saturated samples has increased in heated and unheated conditions. According to Barton (2007), the P wave velocity of a rock is changed with pore volume and the filling material. In water saturated condition the pore filling material is water and in environmental condition most of the pores are filled with air. Therefore high porous rocks increase P wave velocity with water saturation.

Generally it is accepted that saturation does not effect on S wave velocities as shear waves are not transmitting through liquids. Therefore, S wave changes can be due to closure or expansion of cracks in the transmitting direction. Comparison of S wave results with oven drying condition it was

observed the natural samples show a very small lower deviation with oven dried samples (Figure 5 (b)). This is due to the hardening of the rock and therefore closure of cracks creates rock particles to be closer to move the shear wave easily. The S wave velocity of saturated samples which are initially oven dried show lower values than in dry conditions.

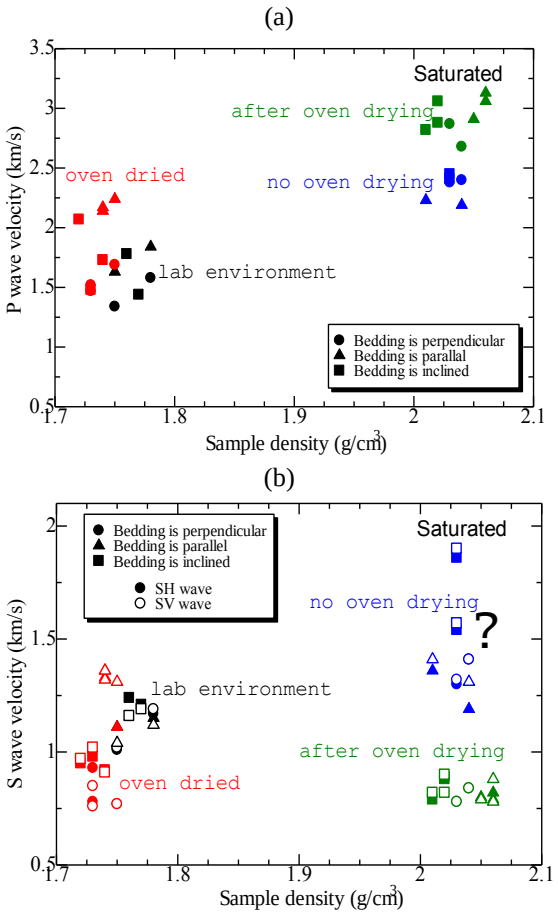

Figure 5 (a) P wave and (b) S wave velocity with density

The graph for V_P versus V_P/V_S in the present study is showed in the Figure 6. The graph shape is most similar to the graph pattern explained by Gueguen and Palciauskas (1994). They explained V_P and V_P/Vs with saturation show a complicated shape and they suggested that this is due to the variation of the densities with fluid saturations.

Considering the packing of quartz spheres it has being accepted the V_P/V_S ratio should be about 1.5 for common rock forming minerals (Castagna et al.. 1984). Further they explained it can be increased for several drying cycles due to the increment of the micro fractures.

In the present study it can be observed the average V_P/V_S ratio for the samples measured in natural environmental conditions is much closer to the predicted previous value (1.5) (Castagna et al., 1984) and it has being increased about to 2 for oven dried samples. Similar result has being obtained for different sandstones by Aktan and Farouq Ali, 1975 (cited in Castagna et al., 1984) considering several cycles of drying. Further, Castagna et al., (1984) indicated the V_P/V_S ratio is increasing with water saturation for different sandstones. In our results also we could observe such increment of the ratio with water saturation. However, it was observed the V_P/V_S ratio is about 3.5 for oven dried and saturated rock samples which is significantly deviated from the other conditions.

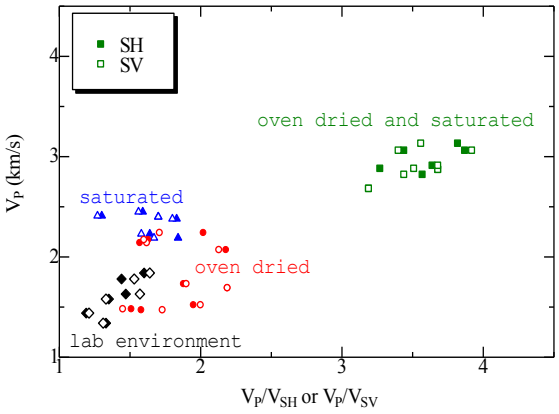

Figure 6 Plot of V_P versus V_P/V_S

Using the above velocities the calculated results (Table 1) indicate a high value of the Young's modulus in parallel to the bedding direction in all conditions. The Poisson's ratio also shows different values with compare to the bedding plane. Poisson's ratio in υ_{13} direction is always high than that of υ_{31} direction. This is comparative with the results of Young's modulus with bedding plane. Despite to the bedding orientation lowest elastic properties are recorded in oven dried and saturated samples.

Young's moduli of natural saturated rock show high values than the oven dried samples and oven dried and saturated samples have the lowest value of Young's moduli within all sample conditions. Therefore it can be assumed the comparative strength of the heated and saturated samples are very less. This can be an effect of further extension of flattened cracks in drying process due to saturation of a rock. Fully water saturation with interconnected pores can weaken the rock. However, high elastic parameters of oven dried samples indicated the rock is hardened by oven drying. Therefore, it needs to consider more on the effect of heating on pore structure by doing the pore structure identification test as explained in section 5.

In contrast, natural water saturated rock shows high elastic moduli than all other samples. It was accepted that the ultrasonic wave velocity measurements are influenced with the properties of fluids and mobility of fluids (Batzle et al., 2006). When seismic wave transmits through a rock, it

will affects the pore fluid pressure and therefore make mobility within the pore fluids. As the time is not enough to adjust for water patches and therefore, fluids concentrated in one point will move with the wave energy and accumulated in one another pore space. Fluid mobility is defined as in Eq. (1) the ratio of permeability (k) of the rock and viscosity of the fluid (η).

$$M = \frac{k}{\eta} \tag{1}$$

The diffusion length for pore water can be expressed as in Eq (2),

$$L = \sqrt{\frac{D}{f}} \tag{2}$$

Where, f is the frequency and D is the diffusivity (Batzle et al., 2006). Therefore, considering mobility M, Bulk modulus of fluid K_f and porosity φ, the diffusion length can be further written as in Eq. (3),

$$L = \sqrt{\frac{M K_{fluid}}{f\phi}} \text{ or } L = \sqrt{\frac{k K_{fluid}}{f\eta\phi}} \tag{3}$$

If the wave length is greater than the fluid diffusion length the water patches of the rock are not in relaxed condition. In this situation the measuring effective bulk modulus is high. Therefore patchy saturation conditions can show stiffer rock conditions than expected in fully saturated and dry conditions. In the present study we obtained high Young's moduli for the natural saturated rock samples which were saturated in vacuum saturator for 72 hours and even though it may be affected with the stiffening of the rock sample with patchy saturations.

Table 1 Dynamic elastic parameters of Tage tuff. 1and 2 directions are along the bedding plane and 3 direction is perpendicular to bedding plane

Parameter		Environ-ment	Saturated rock	Oven dried	Oven dried and saturated
Poisson's ratio					
υ_{12}	υ_{21}	0.15	0.07	0.24	0.46
υ_{13}	υ_{23}	0.06	0.46	0.35	0.51
υ_{31}	υ_{32}	0.05	0.43	0.18	0.42
Young's modulus (GPa)					
E_{33}		3.69	6.62	3.53	3.27
E_{11}	E_{22}	5.10	7.04	6.95	3.95
Shear modulus (GPa)					
G_{12}		2.22	3.29	2.79	1.36
G_{13}	G_{23}	2.07	3.72	1.19	1.40

4. DESICCATION DRIVEN HARDENING

It was observed the P wave velocity is decreasing with saturation showing two different patterns with the orientation of the bedding (Figure 7 (a)). The two different patterns are due to the interconnectivity characteristics of inter-bedding pore water and intra-bedding pore water. When the evaporation occur parallel to the bedding plane P wave velocity decrease gradually until the saturation reach about 70% as inter-bedding pore water is evaporating and keep almost a constant value with intra-bedding pore water evaporation until the saturation reach about 30%. When the evaporation is perpendicular to the bedding plane P wave velocity gradually decrease until the saturation reach about 30%. This is due to the combined evaporation of inter-bedding and intra-bedding pore water.

(a)

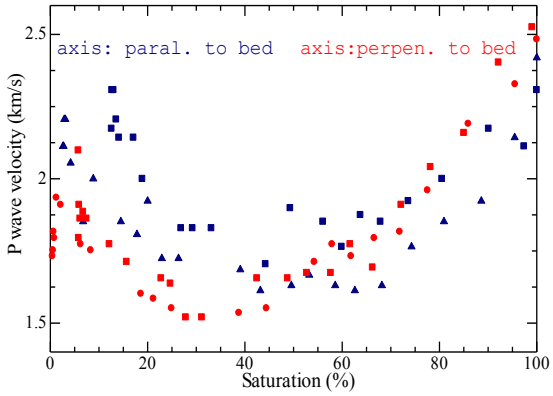

(b)

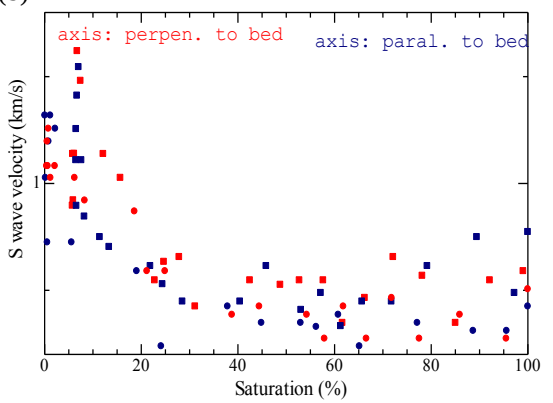

Figure 7 (a) P wave (b) S wave with water saturation

S wave velocity does not show a different graph patterns with compare to the bedding orientation with decreasing saturations (Figure 7 (b)). However, both P wave velocity and S wave velocity gradually increase in below saturation of about 30%.

Normalized sample weight of two sets of samples which used for velocity measurements and strain measurements with time is plotted to identify the weight changes of two comparing samples with time (Figure 8). The normalized weight was

calculated as the change in weight with saturation (g) to the initial volume (cm^3). The small deviations of the normalized weight of samples can be affected with the manual measurements of the velocity. Opening the incubator door may affect the balance reading as well as weight of the velocity measuring sample which is taken out from the incubator.

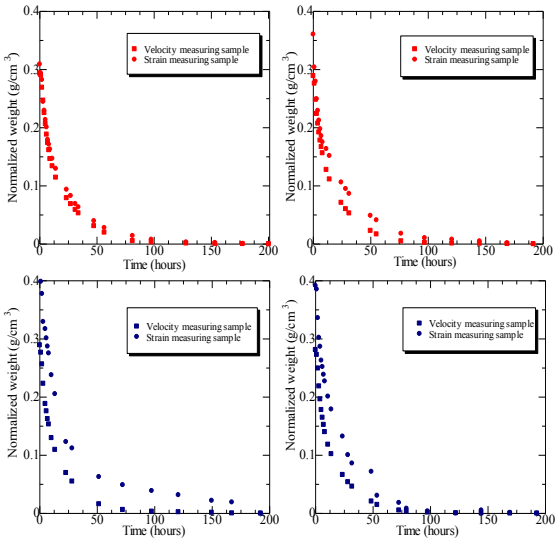

Figure 8 Comparison of weight changes of two samples

The results were comparative with decreasing of volumetric strain measurements in below saturations of around 30% (Figure 9). Negative volumetric strain indicated the contraction of the samples and thus, the experiment identified Tage tuff is contracting in low saturations.

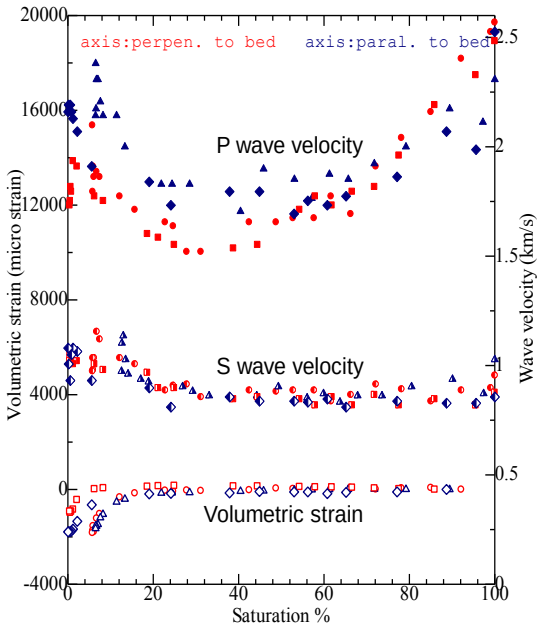

Figure 9 Variation of strain and velocity with saturation

In addition, it was recognized in below saturations of around 30% the relationship of change in P wave velocity and change in volumetric strain follows a shape of a parabola (Figure 10) which can be explained by theories of linear poroelasticity.

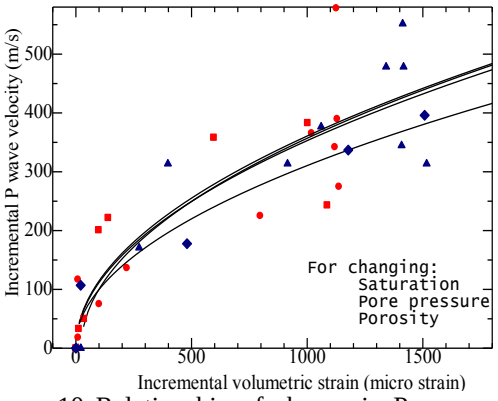

Figure 10 Relationship of change in P wave and change in strain

Considering the Reuss equation for partially saturated rock the velocity V_P was written in Wood's equation as in Eq. (4) (Mavko et al, 2009),

$$V_P = \sqrt{\frac{K_{Average,\mathrm{Re}uss}}{\rho_{sat}}} \tag{4}$$

Where,

$$K_{Average,\mathrm{Re}uss} = \left(\frac{(1-\phi)}{K_{matrix}} + \frac{(S_w)(\phi)}{K_{water}} + \frac{(1-S_w)(\phi)}{K_{gas}} \right)^{-1} \tag{5}$$

$$\rho_{Sat} = \rho_{matrix}(1-\phi) + \rho_{water} S_w \phi + \rho_{gas}(1-S_w)\phi \tag{6}$$

From the linear equation (Eq. 7) the effective pressure can be written as on the rock sample (Gueguen and Palciauskas, 1994, Wang, 1975),

$$P^* = P - \alpha p \tag{7}$$

Where, P is the applied stress and p is the pore water pressure.

From linear poroelastic theories coefficient α is explained as Biot-Willis parameter and it is,

$$\alpha = 1 - \frac{K_{Dry}}{K_{Matrix}} \tag{8}$$

Where K_{Dry} is the skeleton bulk modulus and K_{Matrix} is the solid part bulk modulus.

When the rock is in equilibrium with an applied stress there are two stages can be discussed as

external surface of the solid mass and internal surface of the grains.
For the external surface of the sample Eq. (9),

$$\left(\varepsilon_{kk}\right)^{a} = -\frac{P-p}{K_{Dry}} \tag{9}$$

For internal surface of solid grains it can be written as in Eq. (10),

$$\left(\varepsilon_{kk}\right)^{b} = -\frac{p}{K_{Matrix}} \tag{10}$$

For the equilibrium of the above two stages for the total sample it can written as in Eq. (11),

$$\varepsilon_{kk} = -\frac{P-p}{K_{Dry}} - \frac{p}{K_{Matrix}} \tag{11}$$

In the present study there is no any applied stress on the rock samples. Therefore, if no external hydrostatic pressure *P=0*, and therefore the equation can be re-written as in Eq. (12),

$$\frac{\varepsilon_{kk}}{p} = \frac{1}{K_{Dry}} - \frac{1}{K_{Matrix}} \tag{12}$$

And, the dry bulk modulus can be expressed as in Eq. (13),

$$\frac{1}{K_{Dry}} = \frac{\varepsilon_{kk}}{p} + \frac{1}{K_{Matrix}} \tag{13}$$

If we assume K_{Dry} and $K_{Average,\ Reuss}$ can be compared for low saturations and therefore it can be written as in Eq. (14) ,

$$\frac{\varepsilon_{kk}}{p} + \frac{1}{K_{Matrix}} = \frac{(1-\phi)}{K_{matrix}} + \frac{(S_w)(\phi)}{K_{water}} + \frac{(1-S_w)(\phi)}{K_{gas}} \tag{14}$$

Therefore, considering Wood's equation it can be written the P wave velocity as in Eq. (15),

$$V_P^{\ 2} = \frac{\frac{\varepsilon_{kk}}{p} + \frac{1}{K_{Matrix}}}{\rho_{matrix}(1-\phi) + \rho_{water} S_w \phi + \rho_{gas}(1-S_w)\phi} \tag{15}$$

This equation is similar to an equation of a parabola with axis of V_P and ε_{kk} for changing saturations. It was assumed the changes of pore water pressure, porosity and density of gas are functions of saturation.

5. EFFECT OF TEMPERATURE TO BE DRIED UP

MIP test results indicated the porosity of the samples after drying in different temperatures does not show a significant difference, but pore structure is changing with temperature (Figure 11). High temperature dried samples have about 10% of 4-100 μm pores and that of lab environment samples is about 40%. This may be an effect of fluid (water or water vapor) mobility or surface tension of water which depends on temperature and need to do further analysis for the clarifications.

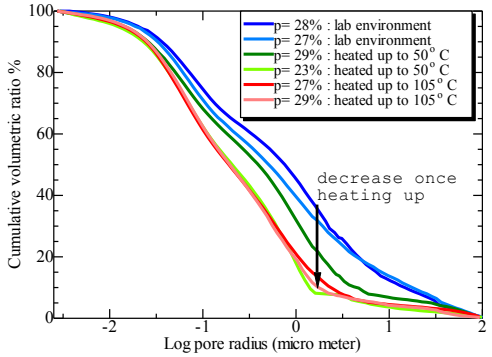

Figure 11 Effect of temperature on MIP results (p=porosity)

6. CONCLUSION

The research was conducted to identify the anisotropic behavior of Tage tuff with changing saturations. Basically two types of experiments were carried out. First study was done to investigate the anisotropic mechanical properties and variations of it in heating and saturation conditions. The second experiment was to identify the relationship between ultrasonic wave velocity variations and strain variations with degree of saturation.

It can be summarized the dynamic mechanical properties of Tage tuff has different values with regards to bedding plane and the effect of water saturation and heating is significant. Heating makes the rock hardening and increase the stiffness and when it saturates the water convert the heated hard rock into weaken. On the other hand, if the rock saturated without heating, water distributed as patches on pore spaces and show stiff characteristics due to patchy saturation.

Concurrent strain and ultrasonic wave velocity measurements were concluded the P wave velocity is decreasing with decreasing saturations and due to the effect of bedding alignment it has two distinguish patterns. On the other hand, S wave velocity is constant with decreasing saturations regardless of the bedding alignment. Bothe P and S wave velocities are increasing in lower saturations of about 30% due to contraction or hardening of the rock sample. In the stage of hardening of the rock or in low water saturations, the change of P wave velocity is related to the change of volumetric strain which can be expressed using the equation 15.

MIP test results indicated heating does not change the porosity, but change the pore size distribution. Heating increase the percentage of smaller cracks (<4μm) and reduce the percentage of larger cracks (>4μm).

Therefore, it can be finalized that heating of a rock sample is hardened the rock by decreasing the size of the larger pores in to smaller pores without changing porosity. This effect changes the elastic properties of Tage tuff which vary with the bedding alignment.

REFERENCES

Adikaram, N.M., Illankoon, T.N., and Osada, M. (2010). Anisotropic behaviour of Tage tuff in 1D drying condition. *Proceedings of twelfth international summer symposium, JSCE,* Japan,187-190.

Aung K.K.S., Osada M., Takahashi M., and Sasaki T. (2008). Characterization of drying-induced deformation behaviour of Opalinus Clay and tuff in no-stress regime. *Environmental Geology,* **58**(6), 1215-1225.

Aung K.K.S., Osada. M. and Thandar Thatoe N.W. (2009). Evaluation and deformation behavior of Shirahama sandstone in moisture transfer process. *Int. J. of the JCRM*, 5, 69-76

Aung K.K.S., Osada. M. and Thandar Thatoe N.W. (2010). Drying-induced deformation behavior of Shirahama sandstone in no loading regime, *Engineering Geology*, **114** (3-4), 423-432.

Barton, N. (2007). *Rock quality, Seismic velocity, Attenuation and Anisotropy.* Taylor & Francis, Nether land.

Batzle, M.L., Han, D.H. and Hofmann, R. (2006). Fluid mobility and frequency dependent seismic velocity-direct measurements. *Geophysics*, **71**(1), N1-N9.

Blatt H., Tracy R.J. and Owens B.E. (2006). *Petrology, Igneous, Sedimentary and Metamorphic*. W.H. Freeman and Company, New York.

Castagna, J.P., Batzle, M.L. and Eastwood, R.L. (1985). Relationship between compressional-wave and shear-wave in clastic silicate rocks. *Geophysics*, **50**(4), 571-581.

Duttine, A, Benedetto, H.D., Bang, D.P.V. and Ezaoui, A. (2007). Anisotropic small strain elastic properties of sands and mixture of sand-clay measured by dynamic and static methods. *Soils and Foundations*, **47**(3), 457-472.

Funatsu T., Seto M., Shimada H., Matsui K. and Kuruppu M. (2004). Combined effects of increasing temperature and confining pressure on the fracture toughness of clay bearing rocks. *Int. J. Rock Mech. & Min. Sci.*, **41**,927-938.

Gueguen, Y. and Palciauskas, V. (1994). *Introduction to the physics of rocks*. Princeton University press, New Jersey.

Ghorbani A., Zamora M. and Cosenza P. (2009). Effects of desiccation on the elastic wave velocities of clay rocks. *Int. J. Rock Mech. & Min. Sci.*, **l46**, 1267-1272.

Kahraman, S. (2007). The correlations between the saturated and dry P wave velocity of rocks. *Ultrasonics*, **46**, 341-348.

King M.S. (1969). Static and dynamic moduli of rocks under pressure, in Someton, W.H., Ed.. *Rock mechanics-theory and practice:* Proc., 11th Sympos. on rock mechanics, Univ. of Calif., Berkeley, 329-351.

King M.S. (2000). Biot dispersion for P and S wave velocities in partially and fully saturated sandstones. *Geophysical Prospecting*, **48**, 1075-1089.

King M.S. (2009). Recent developments in seismic rock physics. *Int J. Rock Mech. & Min. Sci.*, **46**, 1341-1348.

Konstantinova, A.G., Musakina, T.V. and Serikbaev, T.R. (1980). Ultrasonic monitoring of aging and moisture content in rock specimens. *J of Min. Sci.*, **16**, 102-106.

Lo T., Coyner K.B. and Toksoz M.N. (1986). Experimental determination of elastic anisotropy of Berea sandstone, Chicopee shale and Chelmsford granite. *Geophysics*, **51**(1), 164-171.

Mavko G. M., Mukerji T. and Dvorkin J. (2009). *The rock physics handbook*. Cambridge University press. New York.

Murillo, C.A., Thorel, L. and Caicedo, B. (2009). Spectral analysis of surface waves method to assess shear velocity within centrifuge models. *J. of App. Geophy.*, **68**, 135-145.

Okubo, S., Fukui, K. and Gao, X. (2008). Rheological behaviour and model for porous rocks under air-dried and water-saturated condition, *The Open Civil Engineering Journal*, **2**, 88-98.

Okubo S. and Fukui K. (1996). Complete stress-strain curves for various rock types in uniaxial tension. *Int. J. Rock Mech. Min. Sci. & Geomech. Abstr.*, **33**, 549-556.

Sawangsuriya, A., Fall, M. and Fratta, D. (2008). Wave based techniques for evaluation elastic modulus and Poisson's ratio of laboratory compacted lateritic soils. *Geotech Geol.Eng.*, **26**, 567-578.

Song, I., Suh, M., Woo, Y.K. and Hao, T. (2004). Determination of the elastic modulus set of foliated rocks from ultrasonic velocity measurements. *Int. J of Engineering Geology*, **72**, 293-308.

Wang, C., Lin, W. and Wenk, H. (1975). The effects of water and pressure on velocities of elastic waves in a foliated rock. *Geophysics*, **80**, 1065-1069.

Wyllie, M.R.J., Gregory, A.R. and Gardner L.W. (1956). Elastic wave velocities in heterogeneous and porous media. *Geophysics*, **21**, 41-70.